EES Solar

PAPER

View Article Online
View Journal

Cite this: DOI: 10.1039/d5el00166h

Don't fluorinate there! The impact of fluorination position on polymer photostability and its effect on photovoltaic device stability

Joel Luke, [ab] Shiyu Chen,[a] Qiao He, [c] Martina Rimmele, [c] Adam V. Marsh,[b] Alexander J. Gillett, [de] Panagiota Kafourou, [b] Zhuping Fei, [fg] Martin Heeney *[b] and Ji-Seon Kim *[ah]

Despite the excellent progress in organic photovoltaic (OPV) efficiencies, they still suffer from poor operational stability. This is especially true in ambient conditions, with degradation often driven by intrinsic material instabilities. Fluorination of the constituent organic semiconductors, which deepens frontier orbitals and improves organic semiconducting packing, is often utilised to improve photostability. Here, fluorinated analogues of the high-performance workhorse polymer **PBDB-T** are synthesised and their photostability characterised. Device stability, with both Y6 and IT-4F, is found to be critically dependent on the intrinsic polymer photostability, with fluorination of the benzodithiophene (BDT) being particularly ruinous for stability. The co-monomer carbonyl groups in these unstable BDT-fluorinated analogues are found to be highly unstable towards illumination. This instability arises from a disruption of non-covalent interactions along the polymer backbone, where the fluorine on BDT interferes with intramolecular S–O interactions between the thiophene and benzodithiophene-dione (BDD) carbonyl. This leads to increased backbone disorder and a more vulnerable carbonyl environment. These results challenge the conventional belief that fluorination universally improves OPV stability and underscore the crucial role of non-covalent interactions in governing material stability.

Received 9th October 2025
Accepted 1st December 2025

DOI: 10.1039/d5el00166h

rsc.li/EESSolar

Broader context

The global energy transition necessitates a rapid shift from fossil fuels to sustainable alternatives. Among these, solar photovoltaics (PVs) have seen remarkable growth driven by the decreasing cost of silicon solar cells. However, the inherent rigidity, opacity, and fixed bandgap of silicon limit its application in niche applications like built-in photovoltaics (BIPVs), agrivoltaics, and indoor energy harvesting. Organic photovoltaics (OPVs) are a promising and versatile alternative due to their tuneable, semi-transparent, and flexible properties, making them ideal for these niche applications. While recent advances have pushed OPV power conversion efficiencies beyond 20%, their operational stability remains a critical challenge, directly impacting their levelized cost of electricity (LCOE) and market competitiveness. In this study, we attempt to improve the stability of a widely used high-performance organic semiconducting polymer by fluorination. We challenge the conventional wisdom that fluorination universally improves ambient photostability by demonstrating a strong dependency of photostability on the fluorine substitution position, with specific fluorination positions leading to severely compromised photostability. This work provides critical insights into the degradation mechanisms of widely used organic semiconductors and establishes new considerations for the molecular design of more stable OPVs.

[a]*Department of Physics and Centre for Processable Electronics, Imperial College London, Blackett Laboratory, London, SW7 2AZ, UK. E-mail: ji-seon.kim@imperial.ac.uk*

[b]*Physical Sciences and Engineering Division (PSE), King Abdullah University of Science and Technology (KAUST), Thuwal, 23955–6900, Saudi Arabia. E-mail: martin.heeney@kaust.edu.sa*

[c]*Department of Chemistry and Centre for Processable Electronics, Imperial College London, Molecular Sciences Research Hub, White City Campus, London, W12 0BZ, UK*

[d]*Cavendish Laboratory, University of Cambridge, Cambridge, CB3 0HE, UK*

[e]*Department of Physics, Chemistry and Biology (IFM), Linköping University, 581 83 Linköping, Sweden*

[f]*Institute of Molecular Plus, Department of Chemistry, Key Laboratory of Organic Integrated Circuits, Ministry of Education &Tianjin Key Laboratory of Molecular Optoelectronic Science, Tianjin University, Tianjin 300072, China*

[g]*Haihe Laboratory of Sustainable Chemical Transformations, Tianjin 300192, China*

[h]*Department of Chemistry, University of Oxford, Chemistry Research Laboratory, 12 Mansfield Road, Oxford, OX1 3TA, UK*

Introduction

Organic photovoltaics (OPVs) continue to improve in efficiency, now achieving >20% in single-junction cells.[1–3] Despite this, the poor longevity of OPVs remains a considerable barrier towards commercialisation.[4,5] Given the multilayered structure of OPV devices, degradation within any layer or interface is possible.[6] However, the most critical factor for determining device stability is often the photoactive organic layer due to its sensitivity to illumination, particularly in ambient atmospheres.[7–10] Encapsulation mitigates degradation by inhibiting air ingress, yet it only slows the process, highlighting the need for intrinsically stable organic semiconductors (OSCs).[11,12]

One potential strategy that we have suggested as a design rule for improving the stability of OSCs is fluorination.[4] Fluorination is known to deepen a molecule's frontier molecular orbital energy levels, improving the OSC's ambient stability.[13–15] Non-covalent fluorine–sulfur interactions are also known to planarise conjugated backbones,[16–19] potentially inhibiting any conformational changes upon degradation.[7] Fluorination has also been demonstrated to enhance the molecular quadrupole, which is increasingly being used to improve device performance[20] and photostability.[8] Additionally, fluorination often improves the solid-state packing of OSCs, reducing π–π stacking distances and enhancing crystallinity, improving the OSC's morphological and photo-stability.[21–24]

While the **PBDB-T** class of donor polymers,[25,26] particularly **PM6**,[27] have become OPV workhorses due to their excellent efficiencies when paired with the Y-series of acceptors,[27] recent studies have identified the instability of this class of polymers toward ambient illumination. Under illumination in ambient air, we observed a twisting of the polymer backbone, resulting in ultrafast polaron pair formation, which acts as an exciton trap, inhibiting charge transfer and driving device degradation.[9] This degradation mechanism was isolated to the electron-rich benzodithiophene unit, suggesting its use may be problematic in the search for stable OSCs. This has been confirmed by further studies by Prasad *et al.*, who found that the inclusion of the BDT-T linker in Y-series acceptor polymers led to poor ambient photostability.[28]

In this study, we investigate the impact of **PBDB-T** fluorination position on polymer stability to understand if the fluorination strategy can be used to improve the photostability of this important class of polymers. **PBDB-T** is a donor–acceptor copolymer comprised of an electron-rich benzodithiophene (BDT) and an electron-deficient benzodithiophene-dione (BDD) separated by thiophene (T) linkers. Solubilising sidechains of 2-(2-ethylhexyl) thiophene and 2-ethylhexyl are attached to the BDT and BDD units, respectively. We compare the stability of five polymers (chemical structures in Fig. 1) with different positions of fluorination: **PBDB-T** (no fluorine), **PM6** (thiophene sidechain fluorination), **PT-2F** (thiophene spacer fluorination, previously named PFBDB-T),[29] **PBDT-2F** (BDT unit thiophene ring fluorination),and PTDBT-4F (BDT and thiophene linker fluorination).[30] We find fluorination of the thiophene spacers to mildly improve device stability. Interestingly, however, fluorination of the BDT unit itself is disastrous for polymer stability. These findings demonstrate fluorination's potential for improving OPV stability but highlight how sensitive this effect is towards the position of fluorination.

Results and discussion

Polymer properties

PBDB-T and **PM6** were sourced from commercial sources (see Methods), whilst the fluorinated analogues **PT-2F**, and **PTBDT-4F** were synthesised using our previously reported procedures.[29,30] The synthesis of the previously unreported **PBDT-2F** is given in the SI (Fig. S1). The basic properties of the polymers are summarised in Table 1.

The number average molecular weights (M_n) of the polymers were assessed with high temperature (150 °C) gel permeation chromatography (GPC) to avoid aggregation effects. All polymers were in the M_n range of 35–69 kDa and with dispersities ($Đ$) between 2–3.3. Whilst molecular weight is known to impact device performance, these values are within the range previously shown to give consistent device performance for **PBDB-T** and **PM6**, *i.e.* neither very high nor very low.[31,32] Since all polymers have a sufficiently large M_n to be above the effective conjugation length, we believe we can reasonably compare between polymer batches.

The neat polymer film absorption spectra (Fig. S3) show that fluorination along the conjugated backbone slightly narrows

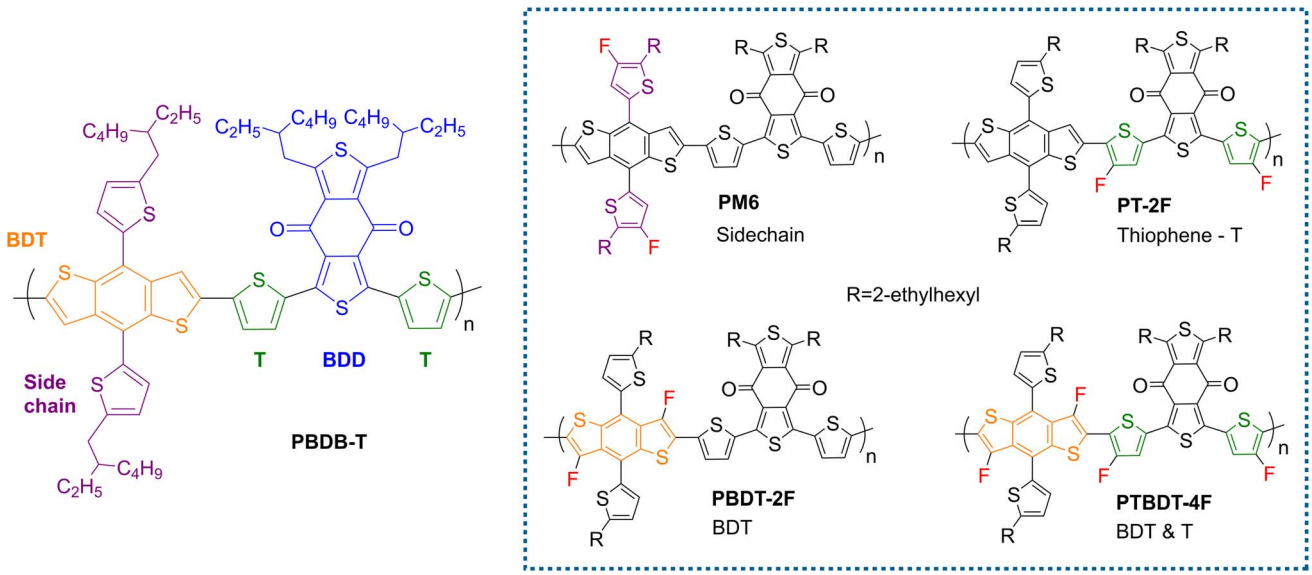

Fig. 1 Chemical structures of the PBDB-T class of polymers studied here with different fluorination positions.

Table 1 An overview of the basic properties of the polymers studied herein. Absorption max ($\lambda_{max,film}$) and optical band gaps ($E_{g,opt,film}$) are extracted from the UV/vis absorption spectra, ionisation energies (IE_{APS}) are extracted from air photoemission spectroscopy (APS), with the LUMO estimated by addition of the IE_{APS} with the $E_{g,opt,film}$. The number-average molecular weight (M_n) is given along with the polydispersity index ($Đ$)

Polymer	$\lambda_{max,film}$/nm	$E_{g,opt,film}$/eV	IE_{APS}/eV	LUMO (IE_{APS} + $E_{g,opt,film}$)/eV	M_n/kDa	$Đ$
PBDB-T	614	1.85	−4.87	−3.02	65	2.3
PM6	618	1.84	−5.06	−3.22	36	2.7
PT-2F	640	1.80	−4.92	−3.12	50	2.0
PBDT-2F	616	1.82	−5.10	−3.28	69	3.3
PTBDT-4F	630	1.80	−5.15	−3.35	47	2.1

the band gap. The lowest energy absorption peak in these polymers correlates to aggregated polymer, as determined by temperature-dependent absorption measurements on solvated **PBDB-T**.[33] This peak shifts 10–20 nm to longer wavelengths for **PT-2F** and **PTBDT-4F**, indicating thiophene fluorination encourages polymer aggregation. Air photoemission spectroscopy (APS) gives the ionisation energy of the polymers (Fig. S4), which is commonly equated with the highest-occupied molecular orbital (HOMO) energy level.[34,35] Fluorination deepens the HOMO level in all cases, the details of which are discussed below.

Polymer photostability

To investigate the photostability of our polymers, we studied neat and blend films before and after 24 hours of photodegradation in air (Fig. S3) with the absorption spectra of **PT-2F** and **PT-2F** : Y6 films shown in Fig. 2. The absorption percentage remaining after degradation of all the polymers is compared in Fig. 2c. Upon ageing, the main absorption peak of **PT-2F** is bleached, with a more pronounced quenching of the low-energy aggregation peak (as determined from previous temperature-dependent studies)[36] and an increase in sub-gap absorption, indicating disrupted polymer packing, more disorder and the emergence of sub-gap states in the degraded polymer. **PBDB-T** and **PM6** also show these features with a similar amount of quenching; however, **PT-2F** maintains a more pronounced aggregation peak following degradation. Surprisingly, within 24 hours, the absorption peaks of **PBDT-2F** and **PTBDT-4F** are nearly entirely bleached. Even after 2 hours of ageing (Fig. S3), the films bleach significantly more than the 24 hours degraded films of the other polymer. Such rapid absorption bleaching reveals a severe instability of these two polymers towards illumination in air. Further, blend film studies (Fig. S7) reveal similar polymer absorption bleaching with a similar trend to the neat films, with **PBDT-2F** and **PTBDT-4F** being the most unstable. The acceptor absorption is also bleached, but to a lesser extent, suggesting that the polymer is the crucial component determining blend stability.

Impact on device stability

To understand how this polymer instability translates to devices, inverted ITO/ZnO/Polymer : Acceptor/MoO_X/Ag solar cells were fabricated with the common acceptors Y6 and IT-4F, which were chosen for their high performance and demonstrated photostability in devices. Device performances are given in Fig. S5. It should be noted that the devices used were not optimised for efficiency, as we wanted to avoid thermal annealing and the use of additives to isolate the effect of polymer selection. As such, the efficiencies are lower than those of similar devices in the literature. With IT-4F, all fluorinated polymers give more efficient devices than **PBDB-T**, demonstrating enhanced open-circuit voltage (V_{OC}) and fill factor (FF). While only the **PT-2F** devices perform superior to the

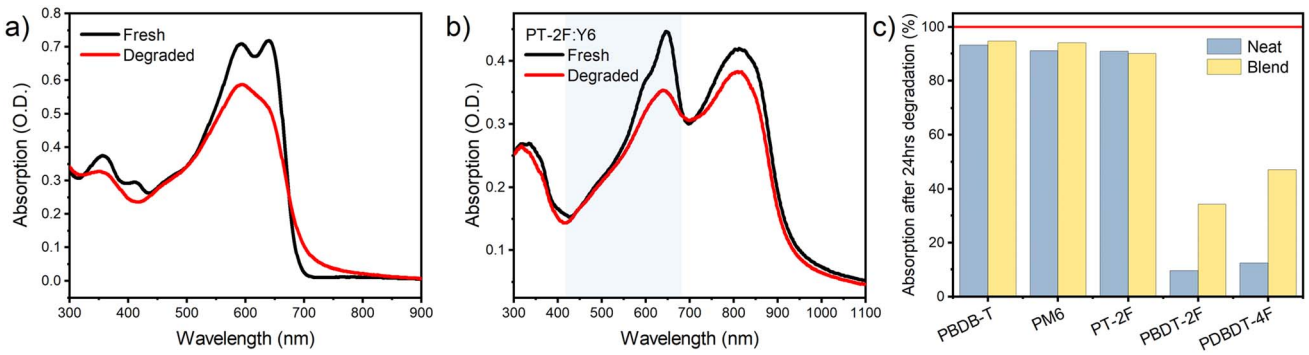

Fig. 2 Film absorption spectra of neat PT-2F (a) and PT-2F blends with Y6 (b) before and after 24 hours of 1 sun illumination in ambient air; (c) the integrated absorption of all neat polymer and Y6-blend films after degradation relative to the fresh absorption; for blend films the blue-shaded area in (b) shows the wavelength range used for integration of the specific polymer absorption.

nonfluorinated polymer when paired with Y6, despite a higher V_{OC} being achieved with all the fluorinated polymers.

These devices were degraded at open circuit under ambient conditions with a white LED at 1 sun light intensity, calibrated by device current matching. The evolution of power conversion efficiency with illumination time is shown in Fig. 3, with full device parameters shown in Fig. S6. Both sets of devices degrade rapidly in air, predominantly driven by a loss of J_{SC}, consistent with our previous reports on **PBDB-T** and **PM6** degradation.[9] The Y6 devices with **PBDB-T**, **PM6**, and **PT-2F** have superior stability to their IT-4F counterparts. With both acceptors, **PT-2F** devices are the most stable, followed by **PBDB-T** and **PM6**, which show similar lifetimes. The unstable polymers **PBDT-2F** and **PTBDT-4F** show the worst device stability, losing nearly all efficiency within 30 minutes of degradation, highlighting the key role of polymer stability in determining the overall device stability. The PCE loss of the different polymer devices after one hour of degradation is compared in Fig. 3c.

Nature of degradation

As in our previous study, we employ transient absorption spectroscopy after 2 hours of film degradation to understand the nature of degradation in the BDT-fluorinated polymers (Fig. S8 and S9). For all fresh polymers, we observe a ground state bleach (GSB) around 600 nm, stimulated emission (SE) 700–750 nm, a broad photoinduced absorption (PIA) centred around 1000 nm assigned to the S_1 state, and a small shoulder feature at 900 nm related to the polymer polaronic absorption, which overlaps with the S_1 PIA. After ageing, **PBDB-T** and **PM6** show a quenched SE band and an enhanced photoinduced absorption (PIA) signal at 900 nm within the first couple of picoseconds, consistent with ultrafast polaron pair formation.[9] Both these signatures are more subtle for **PT-2F**, indicating enhanced stability towards the detrimental formation of trapped polaron pairs. Similarly, upon ageing, **PBDT-2F** and **PTBDT-4F** show SE quenching and an increase in the polaron signal at 900 nm. However, at 1–2 ps, the PIA intensity increases relative to the GSB nearly 3 times compared to **PT-2F** and is also accompanied by a change in the PIA shape. Furthermore, consistent with the steady state absorption measurements, the GSB for **PBDT-2F** and **PTBDT-4F** shows a noticeable blue shift and a near-complete loss of vibronic features. Thus, the TAS data suggest that an additional photophysical process is occurring following degradation of these two polymers.

The common feature distinguishing **PBDT-2F** and **PTBDT-4F** from the other polymers is the fluorination of the BDT unit, which appears to be disastrous for polymer photostability. This has previously been seen in a series of thienothiophene polymers containing fluorinated BDT units.[23] In that study, the accelerated degradation of BDT-fluorinated polymers was assigned to accelerated singlet oxygen [2 + 4] cycloaddition due to differences in internal polarisation. Below, we present energetic, chemical, and computational analyses to investigate potential degradation mechanisms in our polymer series.

Generally, illumination in air is thought to initiate photooxidation in OSCs. Photooxidative stability has been correlated to the energy levels of a material, with deeper frontier energy levels corresponding to enhanced stability.[37] The highest-occupied-molecular-orbital (HOMO) energy levels of the polymers, measured by air photoemission spectroscopy (APS) before and after ageing, are shown in Fig. 4. The HOMO levels of the fresh polymer films are −4.87, −4.92, −5.06, −5.10, and −5.15 eV for **PBDB-T**, **PT-2F**, **PM6**, **PBDT-2F**, and **PTBDT-4F**, respectively. Due to the electronegativity of fluorine, fluorination results in a deepening of HOMO energy levels, with the magnitude of this depending on the number and position of fluorine atoms. We can see that the fluorination on the BDT unit, either on the sidechains as in **PM6** or on the main conjugated backbone, results in the strongest stabilising effect, deepening the HOMO by ~0.2 eV. In comparison, thiophene fluorination only deepens the HOMO level by 0.05 eV. This is understood in terms of the D-A structure of the polymer, where the wavefunction of the HOMO is predominantly localised on the electron-rich donor BDT unit. As such, direct modification of this unit will result in a more substantial effect on the HOMO energy. With the band gap of the polymers being similar, the LUMO levels follow the HOMO trend. Surprisingly, the deeper

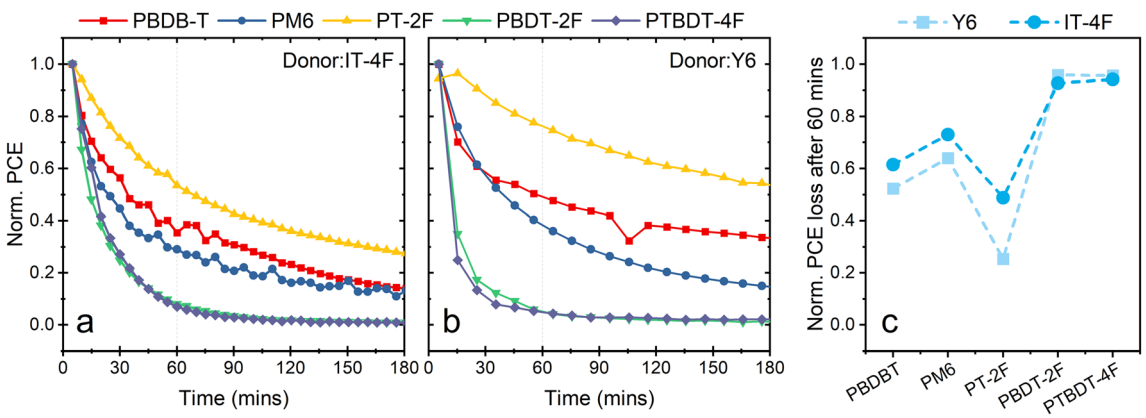

Fig. 3 Device stability of the **PBDB-T** class of polymers. (a & b) Average, normalised power conversion efficiencies (PCE) of ITO/ZnO/Donor : Acceptor/MoO_3/Ag devices as a function of illumination time in air; (c) normalised PCE loss of these devices after 60 minutes ageing.

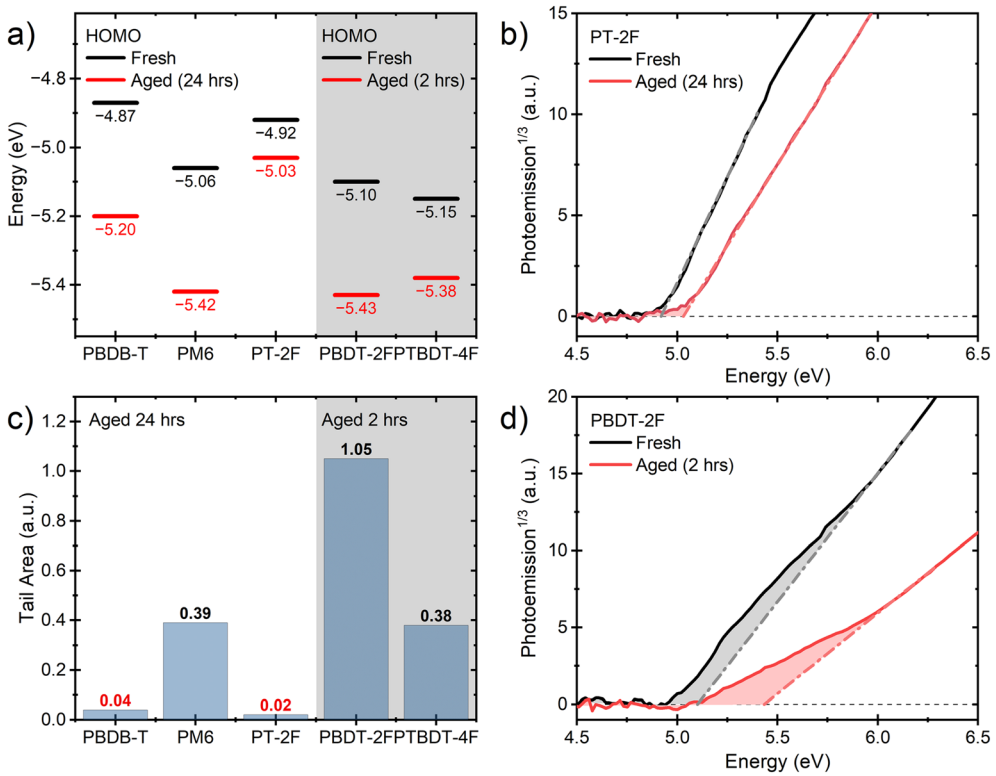

Fig. 4 Energetics of the **PBDB-T** series of polymers. (a) The air photoemission spectroscopy (APS) derived HOMO levels of the polymers before and after ageing; (b) and (d) are examples of the APS spectra obtained for the **PT-2F** and **PBDT-2F** polymers, with their tail area shaded; (c) extracted APS tail areas of polymer films after ageing.

energy levels of the BDT fluorinated polymers do not confer improved ambient photostability.

Following 24 hours of ageing, the HOMO levels of **PBDB-T** and **PM6** are deepened by roughly the same energy ~0.35 eV, whilst **PT-2F** deepens by only 0.11 eV. After 24 hours, the HOMO levels of **PBDT-2F** and **PTBDT-4F** cannot be measured using APS. Still, after 2 hours of ageing, a deepening of 0.33 and 0.18 eV is observed, again showing their relative instability compared to the other polymers. APS is a surface-sensitive technique, so in degraded films, it is particularly sensitive to the most degraded material, *i.e.* the first few nanometres exposed to air. The disrupted conjugation in the degraded polymers widens the bandgap, deepening the HOMO level. In addition to giving the HOMO energy, the tail area of the APS measurements gives an idea about the energetic disorder around the HOMO.[38,39] The tail areas of fresh and aged films are visible in Fig. S4, with extracted values of the aged films summarised in Fig. 4c. Fresh polymer films show that **PBDB-T**, **PM6**, and **PT-2F** have smaller tail areas than **PBDT-2F** and **PTBDT-4F**, indicating that the fresh unstable polymers are more energetically disordered. After ageing, the tail area increases, indicating higher energetic disorder in the degraded polymers. This area is still small for **PBDB-T** and **PT-2F**, slightly larger for **PM6**, and largest for **PBDT-2F** and **PTBDT-4F**, even after only 2 hours of ageing. The deepening of the HOMO energy level and increasing disorder are consistent with UPS studies on fresh and degraded **PBDB-T** presented elsewhere.[28]

PT-2F shows the least change in energetics, with the HOMO only shifting by 0.11 eV. **PT-2F** also maintains the highest relative intensity of the aggregation absorption peak. The more stable aggregation state of **PT-2F** can explain the relative energetic stability, as the most aggregated polymer will have the lowest bandgap and define the HOMO level in the film. AFM images of the more stable polymer films show fibril structures, which are finer for **PT-2F** than **PBDB-T** and **PM6** (Fig. S10). The improved energetic stability and finer morphology may account for the enhanced device stability of **PT-2F** relative to **PBDB-T** and **PM6**, as the finer fibril structure forms a more stable morphology with the acceptor. Photostability is also improved by minor improvements in crystallinity, and therefore, small changes in the polymer or blend morphology may impact photostability.[40] We also note that **PBDT-2F** and **PTBDT-4F** films have less pronounced fibril structure, with this less ordered morphology accounting for the greater energetic disorder observed in these films.

Molecular origin of photodegradation

To understand the molecular origin of polymer degradation in more detail, we used *in situ* Raman spectroscopy with a resonant degradation and probe laser at 514 nm (Fig. S11). Raman peak assignment is consistent with our previously reported assignment of **PBDB-T**.[9] Following extended laser illumination, the Raman intensity of all the polymers is reduced. When normalised, relative peak intensity changes become apparent. For

all the polymers, we see changes consistent with those previously assigned to the photoinduced twisting of the conjugated backbone away from planarity.[9] This is consistent with the TAS data above, which shows polaron pair formation in **PBDB-T**, **PM6**, and **PT-2F**. However, this does not explain the relative instability of the BDT-fluorinated polymers, nor does it reveal an additional degradation mechanism as suggested by the TAS data.

Instead, we turn to FTIR analysis to investigate the products of degradation. The FTIR spectra of fresh and degraded **PT-2F** and **PBDT-2F** are shown in Fig. 5a to represent the stable and unstable polymers, with other polymers shown in Fig. S12–S15. After 1 hour of 1 sun illumination in air, the **PT-2F** is relatively stable, showing only a small reduction in the carbonyl peak at 1648 cm^{-1}, assigned to the BDD unit and the growth of a new, broad peak at 1705 cm^{-1}, likely associated with C=O. Differently, **PBDT-2F** shows a significant reduction in the carbonyl peak, a greater increase of the peak around 1705 cm^{-1}, another possible new carbonyl peak at 1833 cm^{-1}, a new peak at 1190 cm^{-1}, and changes in the C=C fingerprint region. We note that no new broad peaks at higher frequencies (*ca.* 3300 cm^{-1}, Fig. S15) in the degradation product indicate the presence of OH bonds. The significant loss of the BDD carbonyl peak in the unstable polymers indicates that this is the key instability driving the rapid degradation of these polymers.

The broad degraded product peak at 1705 cm^{-1}, observed across all polymers, which we attribute to new carbonyl (C=O) stretching vibrations, is consistent with X-ray photoelectron spectroscopy (XPS) studies on **PBDB-T** that show photooxidation of carbon.[28,41] We note that these studies also indicate direct photooxidation of sulfur at longer degradation times, although this is not apparent in our FTIR analysis. For the more unstable BDT-fluorinated polymers, the additional degraded peaks indicate a new degradation product. The band at 1833 cm^{-1} is unusually high in frequency for a typical carbonyl stretch but may be attributed to an acid anhydride. The anhydride (O=C–O–C=O) is expected to result in two carbonyl peaks due to the symmetric and asymmetric stretches of the two carbonyl groups, with the lower energy symmetric peak being found within the broad carbonyl band around 1705 cm^{-1}. The new absorption at 1190 cm^{-1} could also correspond to the C–O–C stretching mode of an acid anhydride. Alternatively, the high-frequency carbonyl could be the result of an acyl fluoride, and the peak at 1190 cm^{-1} resulting from a sulfone (S=O) stretch vibration. In any case, the new photooxidation product results in a disruption of the conjugated backbone, as demonstrated by the changes in the FTIR C=C fingerprint region, and

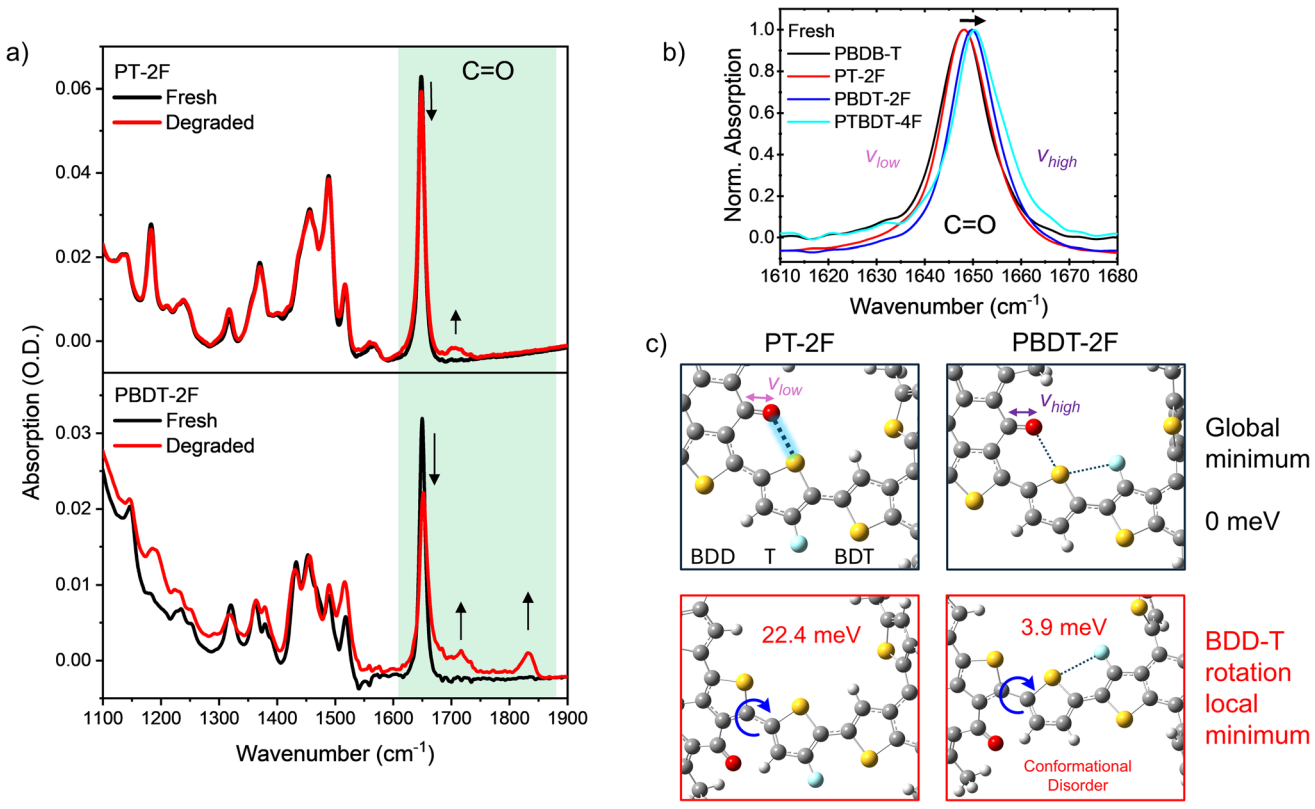

Fig. 5 Chemical degradation analysis. (a) FTIR spectra of **PT-2F** and **PBDT-2F** films on CaF substrates before and after 1 hour of 1 sun illumination in air; (b) FTIR spectra of fresh polymer films normalised to the carbonyl peak; (c) a segment of the energy minimised structure (top) of **PT-2F** (left) and **PBDT-2F** (right) with intramolecular non-covalent interactions between the thiophene sulfur and both the BDD carbonyl and BDT fluorine highlighted with dashed lines. The same polymers (bottom) after BDD-T dihedral rotation to a localised energetic minimum, energies of which are given relative to the global minimum energy structure.

consistent with rapid optical absorption loss and widening bandgap observed above.

Despite not pinpointing the exact degradation product, we have outlined a distinct conjugation-breaking product in the unstable BDT-fluorinated polymers originating from a new degradation pathway. We discuss the origin of this degradation pathway below.

As an observed weak point, we investigate the nature of the carbonyl bonds in the polymer series by plotting the normalised IR carbonyl peak of the fresh polymers in Fig. 5b. The carbonyl peak is shifted to higher frequencies in the BDT-fluorinated polymers, indicating a stronger carbonyl bond. We rationalise this by considering potential non-covalent interactions along the polymer chain. The sulfur in the thiophene spacer unit forms attractive non-covalent interactions with the BDD carbonyl oxygen, driven by electrostatic and dipole interactions.[16] Similarly, S–F electrostatic interactions are possible, although these are weaker than S–O interactions.[16] Nevertheless, with BDT fluorination, the sulfur on the spacer thiophene can form non-covalent interactions with the fluorine on BDT in addition to the S–O interactions with BDD. The competing S–F interaction weakens the S–O interaction, resulting in the stronger carbonyl bond observed with FTIR. The top panels of Fig. 5c depict these interactions as dotted lines, with thickness indicating interaction strength, for the stable **PT-2F** and unstable **PBDT-2F** polymers. We postulate that the S–O interaction stabilises the polymer during photophysical degradation processes, stabilising the polymer conformation and structure. When this interaction is weakened, the polymer becomes more unstable, demonstrating the critical role that molecular structure plays in determining polymer photostability.

Simulations

DFT simulations were performed using Gaussian16 to confirm the impact of BDT-fluorination on the carbonyl group and to investigate the degradation mechanism further.[42] The B3LYP-D3 functional and 6-311G(d,p)++ basis set were utilised to model diffuse orbitals and dispersion effects, which are critical for modelling non-covalent interactions.[43–45] Molecular orbital diagrams on polymer trimers are shown in Fig. S16. HOMOs are delocalised across the conjugated backbone in C=C bonds, while the LUMO is more localised to the BDD-T unit, with fluorination leading to small changes in the degree of LUMO localisation to the BDD unit.

Partial atomic charges are calculated using the electrostatic potential (ESP) method ChelpG, which gives the electrostatic potential on each atom and has been shown to give more consistent results between different basis sets.[16,46] Electrostatic potential surfaces of the polymer monomers are shown in Fig. S17, with localised areas of negative potential concentrated around the electronegative fluorine atoms. The extracted carbonyl oxygen atomic charges are −0.405, −0.404, −0.396 for **PBDB-T**, **PM6**, **PT-2F**, while BDT-fluorination reduces the partial charge of **PBDT-2F** and **PTBDT-4F** to −0.385, and −0.377. The reduced oxygen charge is indicative of a weakened S–O interaction, highlighting the key impact of BDT-fluorination.

The impact of the S–O interaction on polymer conformation is explored through dihedral energy scans of the BDT-T and BDD-T interunit bonds (Fig. S18). It has been previously shown that the degradation of **PM6** can be related to the twisting of the conjugated backbone about these interunit bonds.[9] In the lowest energy conformations of all the polymers, the sulfur of BDT and the thiophene spacer face opposite directions (anti). Fluorination along the backbone planarises the BDT-T linkage with dihedral angles given in Fig. S19. A second local energetic minimum is observed when the BDT-T dihedral angle is again close to planarity, but with the sulfur atoms being syn. The energy of these local minima depends on the polymer, with a detailed explanation outlined in Fig. S18. **PBDB-T** and **PTBDT-4F** have relatively high local minima (60 meV), while **PT-2F** and **PBDT-2F** have local minima only 15–18 meV above the global minima. These energetic differences show no correlation with the polymer stability trend observed and, therefore, cannot explain the degradation mechanism of BDT-fluorinated polymers.

Now, focusing on the BDD-T dihedral, we expect the S–O interactions to play a more critical role. Rotation about this dihedral is shown in Fig. 5c for **PT-2F** and **PBDT-2F**. The minimum energy structure (Fig. 5c, top panels) in all polymers is when the sulfur of the thiophene spacer and carbonyl of BDD are on the same side, with a dihedral angle of ∼15°. Rotation about the BDD-T dihedral by ∼180° results in a second local minimum when the spacer thiophene sulfur and BDD carbonyl are anti (Fig. 5c, bottom panels). For **PBDB-T** and **PT-2F** these minima are 20 meV higher in energy than the global minimum, demonstrating the stabilising effect of the S–O interaction when the sulfur and carbonyl are syn. In the BDT-fluorinated polymers, the barrier to BDD-T rotation is lower, and the local anti-minima are <5 meV above the global minimum, demonstrating weaker S–O stabilisation. The lower rotation barrier and energetic similarity between the syn and anti-conformers in the BDT-fluorinated polymers will result in conformational and structural disorder in the polymer. This is consistent with the increased energetic disorder of the BDT-fluorinated polymers as measured by APS and the less pronounced fibril structure in AFM images. It also highlights the impact of BDT-fluorination on weakening the S–O non-covalent interaction, corroborating our experimental evidence that BDT-fluorination affects the BDD carbonyl.

Sidechain-driven degradation has been demonstrated to be a key degradation pathway through both photooxidation[41] and photophysical processes such as homolytic fission of C–C bonds and H abstraction.[47] The likelihood of these photophysical processes occurring can be interrogated by calculating the Laplacian bond order (LBO) of the labile bonds, which we detail for our polymer series in Fig. S20 and S21.[47,48] All polymers show similar LBOs for all the bonds considered, indicating that the differences in sidechain stability cannot account for the dramatic differences we observe in photostability. Considering photooxidation, XPS analysis has suggested that **PBDB-T** undergoes alkyl-sidechain photooxidation.[41] However, the pronounced loss of conjugation observed in the absorption spectra and energetic degradation of the unstable BDT-

fluorinated polymers, together with the C=C peak changes in the FTIR spectra, indicate that photooxidation is more probably occurring on the conjugated backbone.

Photooxidation can proceed *via* the photoinduced formation of reactive oxygen species, such as superoxide or singlet oxygen.[14] Superoxide can be formed following photoinduced electron transfer from the LUMO of an OSC to molecular oxygen. The single reduction potential of O_2 is −4.11 eV,[49] meaning superoxide formation following electron transfer from the LUMO of any of the polymers is thermodynamically favourable and cannot be used to rationalise the observed stability trend.

Singlet oxygen formation occurs *via* energy transfer from triplet states in the OSC. Once formed, singlet oxygen acts as an electrophile, attacking the electron-rich conjugated backbone through cycloaddition reactions. A [2 + 2] cycloaddition of the BDT thiophene ring has been proposed as a degradation pathway in **PBDB-T**.[50] In the present case, however, fluorination is expected to deactivate the BDT thiophene towards such electrophilic attack. Beyond the substituted ring, fluorination impacts the electron distribution along the conjugated backbone and may influence the reactivity of other units towards singlet-oxygen attack. A previous study employing partial charge analysis reported that fluorination of the BDT unit accelerates singlet oxygen [2 + 4] cycloaddition of the thienothiophene comonomer due to an increase in local electron density.[23] We performed an equivalent analysis of our polymer series using the ChelpG method introduced above (Fig. S22). The analysis focused on the electro-negativity of the α-carbons on the BDT thiophene ring, the thiophene linker, and the thiophene of BDD unit, identified as potential sites for [2 + 4] cycloaddition. In fluorinated polymers, the α-carbon closest to the fluorination site becomes more electron-rich; however, the impact on adjacent thiophene rings is less systematic, showing no clear correlation with the observed stability trend. These results indicate that the initial reactivity towards singlet oxygen alone cannot account for the differences in stability we observe.

To shine further light on the degradation mechanism, we investigated the impact of the atmosphere on photodegradation. Here, polymer films were illuminated in an inert N_2 atmosphere, and their absorption spectra were measured (Fig. S23). After 24 h illumination, **PBDB-T**, **PM6**, and **PT-2F** absorption showed minimal changes, while **PBDT-2F** and **PTBDT-4F** demonstrated clear bleaching, albeit at a slower rate than photodegradation in air. This suggests that the instability of the BDT-fluorinated polymers is an intrinsic instability to illumination, which is accelerated by oxygen. Although this does not exclude the possibility of a singlet oxygen attack, it suggests an instability within the polymer itself. Based on this, we postulate that a photophysical change along the conjugated backbone is an important degradation mechanism. This change could be a photo-induced ring-opening,[51] a photo-isomerisation,[52] or bond scission; we discuss these possibilities in more detail in SI Note 1. The S–O non-covalent interaction then provides a scaffolding for the molecular conformation and structure, either resisting initial photophysical changes or facilitating the reformation of the ground-state polymer structure without further reactions or conjugation loss. When this interaction is weakened by competing S–F interactions, the initial photophysical change is more likely to be followed by further irreversible chemical changes, either through isomeric reorganisation or interactions with external species, resulting in new degradation products and a loss of backbone conjugation.

Conclusion

Our data suggests that BDT-fluorination severely compromises the photostability of **PBDB-T** polymers, which is critical for device photostability. Upon degradation BDT-fluorinated polymers exhibit an additional degradation mechanism centred on the carbonyl bonds in the BDD unit. We have provided experimental evidence of a different C=O environment in BDT-fluorinated polymers. Through a combination of simulations, we assign this to the disruption of the intramolecular S–O non-covalent interaction between thiophene and BDD by competing S–F interactions between the thiophene and BDT in BDT-fluorinated polymers. Weakening the S–O interaction results in more backbone structural disorder and a propensity to conjugation loss upon illumination. We hypothesise that weakening the intramolecular S–O non-covalent interactions makes the polymer more prone to irreversible photophysical changes. Strong S–O interactions act as a structural scaffold, inhibiting photophysical changes such as isomerisation or facilitating reformation of the initial structure following, say, photoinduced ring-opening. Without this stabilising template, the ring-opening process leads to further irreversible reactions, such as isomerisation or reactions with environmental species.

In general, the role of these non-covalent interactions is challenging to decipher due to the lack of direct experimental techniques, the various computational methods available, and the inherent energetic and structural disorder in organic semiconducting polymers. Further work in this area is required to develop tools to characterise these non-covalent interactions and apply these to the applied challenges in organic semiconductors.

Our results highlight the impact of fluorination position on polymer photostability, challenging the general assumption that fluorination always enhances stability through improved packing and deeper energy levels. We demonstrate that the key non-covalent interactions in fluorinated **PBDB-T** polymers are not S–F interactions but rather S–O interactions between the thiophene and BDD. Destabilising these S–O interactions can severely compromise photostability, highlighting a crucial molecular design rule when utilising the commonly employed BDD unit. More generally, the fluorination position should be chosen to avoid disrupting planarizing non-covalent interactions. Fluorination, therefore, is not a one-size-fits-all solution for improving polymer stability, as it can influence other intermolecular interactions along the polymer backbone. We do not want to discourage the use of fluorination to improve efficiency, but emphasise that new OPV materials, particularly fluorinated analogues, should be screened for photostability through basic photobleaching experiments.

Conflicts of interest

The authors declare no conflicts of interest.

Data availability

Data for this article, comprising all the data used to make the figures in the article and supplementary information (SI), as well as the Gaussian output files from simulations, are available at the Open Science Framework at https://osf.io/e9wjn/. The project will be made public upon acceptance for publication. Supplementary information is available. See DOI: https://doi.org/10.1039/d5el00166h.

Acknowledgements

The authors would like to acknowledge the UK Engineering and Physical Sciences Research Council for funding through both the Application Targeted and Integrated Photovoltaics programme grant (EP/T028513/1) and the Centre for Doctoral Training in Plastic Electronic Materials (EP/L016702/1). Additionally, J. L, A. V. P, P. K. and M. H. thank the King Abdullah University of Science and Technology (KAUST) under award (ORFA-CRG11-2022-5045). A. J. G. thanks the Leverhulme Trust for an Early Career Fellowship (ECF-2022-445), the Knut and Alice Wallenberg Foundation for a Wallenberg Academy Fellows award (KAW 2023.0082), and the Swedish Research Council (VR) for a Starting Grant (2024-03915).

References

1 L. Zhu, M. Zhang, Z. Zhou, W. Zhong, T. Hao, S. Xu, *et al.*, Progress of organic photovoltaics towards 20% efficiency, *Nat. Rev. Electr. Eng.*, 2024, **1**(9), 581–596.

2 N. Wei, J. Chen, Y. Cheng, Z. Bian, W. Liu, H. Song, *et al.*, Constructing Multiscale Fibrous Morphology to Achieve 20% Efficiency Organic Solar Cells by Mixing High and Low Molecular Weight D18, *Adv. Mater.*, 2024, **36**(41), e2408934.

3 M. Du, N. Sun, H. Cheng, X. Liu, X. Yi, Q. Guo, *et al.*, Multiple-Birth-Acceptor: Easily-Synthesized Mixture for Easily-Fabricated Quaternary Organic Solar Cells with Beyond 20% Efficiency, *Angew Chem. Int. Ed. Engl.*, 2025, e202515114.

4 J. Luke, E. J. Yang, C. Labanti, S. Y. Park and J. S. Kim, Key molecular perspectives for high stability in organic photovoltaics, *Nat. Rev. Mater.*, 2023, **8**(12), 839–852.

5 P. Ding, D. Yang, S. Yang and Z. Ge, Stability of organic solar cells: toward commercial applications, *Chem. Soc. Rev.*, 2024, **53**(5), 2350–2387.

6 M. H. Wu, B. Ma, S. S. Li, J. Q. Han and W. C. Zhao, Powering the Future: A Critical Review of Research Progress in Enhancing Stability of High-Efficiency Organic Solar Cells, *Adv. Funct. Mater.*, 2023, **33**(50), 2305445.

7 J. Luke, E. M. Speller, A. Wadsworth, M. F. Wyatt, S. Dimitrov, H. K. H. Lee, *et al.*, Twist and Degrade-Impact of Molecular Structure on the Photostability of Nonfullerene Acceptors and Their Photovoltaic Blends, *Adv. Energy Mater.*, 2019, **9**(15), 1803755.

8 J. Luke, E. J. Yang, Y. C. Chin, Y. X. Che, L. Winkler, D. Whatling, *et al.*, Strong Intermolecular Interactions Induced by High Quadrupole Moments Enable Excellent Photostability of Non-Fullerene Acceptors for Organic Photovoltaics, *Adv. Energy Mater.*, 2022, **12**(30), 2201267.

9 Y. W. Wang, J. Luke, A. Privitera, N. Rolland, C. Labanti, G. Londi, *et al.*, The critical role of the donor polymer in the stability of high-performance non-fullerene acceptor organic solar cells, *Joule*, 2023, **7**(4), 810–829.

10 A. J. Clarke, J. Luke, R. Meitzner, J. Y. Wu, Y. M. Wang, H. K. H. Lee, *et al.*, Non-fullerene acceptor photostability and its impact on organic solar cell lifetime, *Cell Rep. Phys. Sci.*, 2021, **2**(7), 100498.

11 E. Planes, S. Juillard, M. Matheron, N. Charvin, S. Cros, D. P. Qian, *et al.*, Encapsulation Effect on Performance and Stability of Organic Solar Cells, *Adv. Mater. Interfaces*, 2020, **7**(15), 2000293.

12 J. Adams, M. Salvador, L. Lucera, S. Langner, G. D. Spyropoulos, F. W. Fecher, *et al.*, Water Ingress in Encapsulated Inverted Organic Solar Cells: Correlating Infrared Imaging and Photovoltaic Performance, *Adv. Energy Mater.*, 2015, **5**(20), 1501065.

13 V. N. Viswanathan, A. J. Ferguson, J. R. Pfeilsticker, B. W. Larson, L. E. Garner, C. P. Brook, *et al.*, Strategic fluorination of polymers and fullerenes improves photostability of organic photovoltaic blends, *Org. Electron.*, 2018, **62**, 685–694.

14 E. M. Speller, A. J. Clarke, N. Aristidou, M. F. Wyatt, L. Francas, G. Fish, *et al.*, Toward Improved Environmental Stability of Polymer:Fullerene and Polymer:Nonfullerene Organic Solar Cells: A Common Energetic Origin of Light- and Oxygen-Induced Degradation, *ACS Energy Lett.*, 2019, **4**(4), 846–852.

15 T. Hodsden, K. J. Thorley, J. Panidi, A. Basu, A. V. Marsh, H. J. Dai, *et al.*, Core Fluorination Enhances Solubility and Ambient Stability of an IDT-Based n-Type Semiconductor in Transistor Devices, *Adv. Funct. Mater.*, 2020, **30**(17), 2000325.

16 K. J. Thorley and I. McCulloch, Why are S–F and S–O non-covalent interactions stabilising?, *J. Mater. Chem. C*, 2018, **6**(45), 12413–12421.

17 P. Boufflet, Y. Han, Z. Fei, N. D. Treat, R. Li, D. M. Smilgies, *et al.*, Using Molecular Design to Increase Hole Transport: Backbone Fluorination in the Benchmark Material Poly(2,5-bis(3-alkylthiophen-2-yl)thieno[3,2-b]-thiophene) (pBTTT), *Adv. Funct. Mater.*, 2015, **25**(45), 7038–7048.

18 W. Li, S. Albrecht, L. Yang, S. Roland, J. R. Tumbleston, T. McAfee, *et al.*, Mobility-controlled performance of thick solar cells based on fluorinated copolymers, *J. Am. Chem. Soc.*, 2014, **136**(44), 15566–15576.

19 T. Xu and L. Yu, How to design low bandgap polymers for highly efficient organic solar cells, *Mater. Today*, 2014, **17**(1), 11–15.

20 T. Dai, Y. Meng, Z. Wang, J. Lu, Z. Zheng, M. Du, *et al.*, Modulation of Molecular Quadrupole Moments by Phenyl

Side-Chain Fluorination for High-Voltage and High-Performance Organic Solar Cells, *J. Am. Chem. Soc.*, 2025, **147**(5), 4631–4642.

21 Z. D. Li, T. Zhang, Y. Xin, X. L. Zhao, D. L. Yang, F. Wu, *et al.*, Synergistic effect of fluorination and regio-regularity on the long-term thermal stability of polymer solar cells, *J. Mater. Chem. A*, 2016, **4**(47), 18598–18606.

22 Z. Hu, R. T. Haws, Z. Fei, P. Boufflet, M. Heeney, P. J. Rossky, *et al.*, Impact of backbone fluorination on nanoscale morphology and excitonic coupling in polythiophenes, *Proc. Natl. Acad. Sci. U. S. A.*, 2017, **114**(20), 5113–5118.

23 H. J. Son, W. Wang, T. Xu, Y. Y. Liang, Y. E. Wu, G. Li, *et al.*, Synthesis of Fluorinated Polythienothiophene-benzodithiophenes and Effect of Fluorination on the Photovoltaic Properties, *J. Am. Chem. Soc.*, 2011, **133**(6), 1885–1894.

24 L. Yang, J. R. Tumbleston, H. Zhou, H. Ade and W. You, Disentangling the impact of side chains and fluorine substituents of conjugated donor polymers on the performance of photovoltaic blends, *Energy Environ. Sci.*, 2013, **6**(1), 316–326.

25 L. Ye, X. Jiao, M. Zhou, S. Zhang, H. Yao, W. Zhao, *et al.*, Manipulating aggregation and molecular orientation in all-polymer photovoltaic cells, *Adv. Mater.*, 2015, **27**(39), 6046–6054.

26 Z. Zheng, H. Yao, L. Ye, Y. Xu, S. Zhang and J. Hou, PBDB-T and its derivatives: A family of polymer donors enables over 17% efficiency in organic photovoltaics, *Mater. Today*, 2020, **35**, 115–130.

27 M. Zhang, X. Guo, W. Ma, H. Ade and J. Hou, A Large-Bandgap Conjugated Polymer for Versatile Photovoltaic Applications with High Performance, *Adv. Mater.*, 2015, **27**(31), 4655–4660.

28 S. Prasad, Z. Genene, C. F. N. Marchiori, S. Singh, L. K. E. Ericsson, E. Wang, *et al.*, Effect of molecular structure on the photochemical stability of acceptor and donor polymers used in organic solar cells, *Mater. Adv.*, 2024, **5**(19), 7708–7720.

29 Z. Fei, F. D. Eisner, X. Jiao, M. Azzouzi, J. A. Rohr, Y. Han, *et al.*, An Alkylated Indacenodithieno[3,2-b]thiophene-Based Nonfullerene Acceptor with High Crystallinity Exhibiting Single Junction Solar Cell Efficiencies Greater than 13% with Low Voltage Losses, *Adv. Mater.*, 2018, **30**(8), 1800728.

30 F. D. Eisner, M. Azzouzi, Z. Fei, X. Hou, T. D. Anthopoulos, T. J. S. Dennis, *et al.*, Hybridization of Local Exciton and Charge-Transfer States Reduces Nonradiative Voltage Losses in Organic Solar Cells, *J. Am. Chem. Soc.*, 2019, **141**(15), 6362–6374.

31 X. M. Zheng, H. Lu, S. Y. Feng, R. Hou, W. L. Liu, S. L. Ming, *et al.*, Effect of polymer molecular weight and processing solvent on the morphology and photovoltaic performance of inverted non-fullerene solar cells, *Dyes Pigm.*, 2021, **194**, 109560.

32 Q. Liu, J. Fang, J. Wu, L. Zhu, X. Guo, F. Liu, *et al.*, Tuning Aggregation Behavior of Polymer Donor viaMolecular-Weight Control for Achieving 17.1% Efficiency Inverted Polymer Solar Cells, *Chin. J. Chem.*, 2021, **39**(7), 1941–1947.

33 D. P. Qian, L. Ye, M. J. Zhang, Y. R. Liang, L. J. Li, Y. Huang, *et al.*, Design, Application, and Morphology Study of a New Photovoltaic Polymer with Strong Aggregation in Solution State, *Macromolecules*, 2012, **45**(24), 9611–9617.

34 Y. C. Chin, M. Daboczi, C. Henderson, J. Luke and J. S. Kim, Suppressing PEDOT:PSS Doping-Induced Interfacial Recombination Loss in Perovskite Solar Cells, *ACS Energy Lett.*, 2022, **7**(2), 560–568.

35 Y. Fu, T. H. Lee, Y. C. Chin, R. A. Pacalaj, C. Labanti, S. Y. Park, *et al.*, Molecular orientation-dependent energetic shifts in solution-processed non-fullerene acceptors and their impact on organic photovoltaic performance, *Nat. Commun.*, 2023, **14**(1), 1870.

36 J. Hou, O. Inganas, R. H. Friend and F. Gao, Organic solar cells based on non-fullerene acceptors, *Nat. Mater.*, 2018, **17**(2), 119–128.

37 E. M. Speller, A. J. Clarke, J. Luke, H. K. H. Lee, J. R. Durrant, N. Li, *et al.*, From fullerene acceptors to non-fullerene acceptors: prospects and challenges in the stability of organic solar cells, *J. Mater. Chem. A*, 2019, **7**(41), 23361–23377.

38 M. Daboczi, I. Hamilton, S. Xu, J. Luke, S. Limbu, J. Lee, *et al.*, Origin of Open-Circuit Voltage Losses in Perovskite Solar Cells Investigated by Surface Photovoltage Measurement, *ACS Appl. Mater. Interfaces*, 2019, **11**(50), 46808–46817.

39 S. Lee, D. B. Kim, I. Hamilton, M. Daboczi, Y. S. Nam, B. R. Lee, *et al.*, Control of Interface Defects for Efficient and Stable Quasi-2D Perovskite Light-Emitting Diodes Using Nickel Oxide Hole Injection Layer, *Adv. Sci.*, 2018, **5**(11), 1801350.

40 E. J. Yang, J. Luke, Y. Fu, Z. R. Qiao, M. Bidwell, A. V. Marsh, *et al.*, Unraveling the Impact of Solution Filtration on Organic Solar Cell Stability, *Adv. Funct. Mater.*, 2024, **34**(42), 2406941.

41 M. A. Anderson, A. Hamstra, B. W. Larson and E. L. Ratcliff, Distinguishing photo-induced oxygen attack on alkyl chain conjugated backbone for alkylthienyl-benzodithiophene (BDTT)-based push-pull polymers, *J. Mater. Chem. A*, 2023, **11**(33), 17858–17871.

42 M. J. Frisch, G. W. Trucks, H. B. Schlegel, G. E. Scuseria, M. A. Robb and J. R. Cheeseman, *et al.*, *Gaussian 16 Rev. C.01*, Wallingford, CT, 2016.

43 E. F. Grossman, D. A. Daramola and G. G. Botte, Comparing B3LYP and B97 Dispersion-corrected Functionals for Studying Adsorption and Vibrational Spectra in Nitrogen Reduction, *ChemistryOpen*, 2021, **10**(3), 316–326.

44 A. D. Becke, Density-functional thermochemistry. III. The role of exact exchange, *J. Chem. Phys.*, 1993, **98**(7), 5648–5652.

45 P. J. Stephens, F. J. Devlin, C. F. Chabalowski and M. J. Frisch, Ab-Initio Calculation of Vibrational Absorption and Circular-Dichroism Spectra Using Density-Functional Force-Fields, *J. Phys. Chem.*, 1994, **98**(45), 11623–11627.

46 C. M. Breneman and K. B. Wiberg, Determining Atom-Centered Monopoles from Molecular Electrostatic

Potentials - the Need for High Sampling Density in Formamide Conformational-Analysis, *J. Comput. Chem.*, 1990, **11**(3), 361–373.

47 H. Xu, J. H. Han, M. Babics, L. Huerta Hernandez, D. Rosas Villalva, M. Sanviti, *et al.*, Elucidating the photodegradation pathways of polymer donors for organic solar cells with seven months of outdoor operational stability, *Nat. Photonics*, 2025, **19**(4), 415–425.

48 T. Lu and F. W. Chen, Bond Order Analysis Based on the Laplacian of Electron Density in Fuzzy Overlap Space, *J. Phys. Chem. A*, 2013, **117**(14), 3100–3108.

49 Y. A. Ilan, G. Czapski and D. Meisel, The one-electron transfer redox potentials of free radicals. I. The oxygen/superoxide system, *Biochim. Biophys. Acta*, 1976, **430**(2), 209–224.

50 S. Kim, M. A. Rashid, T. Ko, K. Ahn, Y. Shin, S. Nah, *et al.*, New Insights into the Photodegradation Mechanism of the PTB7-Th Film: Photooxidation of π-Conjugated Backbone upon Sunlight Illumination, *J. Phys. Chem. C*, 2020, **124**(5), 2762–2770.

51 M. N. R. Ashfold, M. Bain, C. S. Hansen, R. A. Ingle, T. N. V. Karsili, B. Marchetti, *et al.*, Exploring the Dynamics of the Photoinduced Ring-Opening of Heterocyclic Molecules, *J. Phys. Chem. Lett.*, 2017, **8**(14), 3440–3451.

52 Y. Che, M. R. Niazi, R. Izquierdo and D. F. Perepichka, Mechanism of the Photodegradation of A-D-A Acceptors for Organic Photovoltaics, *Angew Chem. Int. Ed. Engl.*, 2021, **60**(47), 24833–24837.